Three-photon electromagnetically induced absorption in a ladder-type atomic system

Han Seb Moon* and Taek Jeong
Department of Physics, Pusan National University, Busan 609-735, Korea
(Received 5 November 2013; published 12 March 2014)

We report on three-photon electromagnetically induced absorption (TPEIA) due to three-photon coherence in ladder-type atomic systems for the $5S_{1/2}$-$5P_{3/2}$-$5D_{5/2}$ transition in ^{87}Rb atoms. When a counterpropagating coupling field was added to the typical ladder-type electromagnetically induced transparency (EIT) experiment, both EIT and two-photon absorption (TPA) switched to TPEIA. Considering three-photon coherence in a Doppler-broadened three-level ladder-type atomic system, the spectrum of the switch from EIT and TPA to TPEIA was numerically calculated and could be understood by decomposing the calculated spectrum into two-photon coherence and three-photon coherence components.

DOI: 10.1103/PhysRevA.89.033822 PACS number(s): 42.50.Gy, 32.80.Qk, 32.80.Wr

I. INTRODUCTION

Electromagnetically induced transparency (EIT) and electromagnetically induced absorption (EIA) are widely regarded as important phenomena resulting from two-photon coherence [1–4]. EIT is a destructive quantum interference phenomenon due to two-photon coherence in a three-level atomic system. On the other hand, EIA is a consequence of the transfer of coherence when the two-photon coherence between degenerate excited levels is transferred spontaneously to degenerate ground levels [4–6]. The narrow resonance of EIT or EIA has been applied to atomic clocks, atomic magnetometers, the frequency stabilization of lasers, and the manipulation of the speed of light pulses [7–11].

Two-photon coherence phenomena in a ladder-type atomic system have received relatively little attention compared with those in a Λ-type atomic system [12–17]. Despite this fact, EIT in the ladder-type atomic system exhibits interesting differences in its spectral features and applications [13–17]. When a weak probe laser and a strong coupling laser overlap through an atom vapor cell, the EIT and two-photon absorption (TPA) spectra due to two-photon coherence were observed in a ladder-type atomic system [18]. However, since the effect of EIA in atomic media was experimentally discovered in a degenerate two-level atomic system that consists of at least 12 Zeeman levels [4], the EIA effect was modeled and explained using ground-state coherence transfer in an N-type energy-level configuration [5,6]. In addition, the conversion of EIT into EIA by ground-state coherence transfer was demonstrated [19]. This mechanism cannot occur in ladder-type three-level atomic systems.

However, if another laser is added to the atomic medium considering two-photon coherence, it is necessary to consider multiphoton effects. When a weak probe laser and two counterpropagating coupling lasers interacted with a three-level Λ-type atomic vapor, absorption phenomena were observed in an atomic coherent medium with two counterpropagating coupling lasers; this observation differs from EIT due to two-photon coherence with a coupling laser [20–25]. In addition, the comblike spectra of new fields generated in EIA media have been reported [26,27]. Although multiphoton coherence phenomena in a three-level Λ-type or degenerate two-level atomic system have been studied, there are no reports examining narrow three-photon absorption in the ladder-type atomic system. In this work we report our observation of an enhanced absorption signal due to three-photon coherence in hyperfine structure based on ladder-type atomic systems when a coupling laser is added to the atomic medium under the condition of EIT or TPA due to two-photon coherence.

In this paper, we investigate three-photon EIA in three-level ladder-type Doppler-broadened atomic systems. When a counterpropagating coupling field is added to the configuration for typical ladder-type EIT, we can experimentally demonstrate the transformation of EIT into Doppler-free three-photon absorption in the $5S_{1/2}$-$5P_{3/2}$-$5D_{5/2}$ transition of ^{87}Rb. The spectrum of three-photon absorption is numerically calculated in a simple three-level atomic system considering three-photon coherence. To clarify the effects of three-photon coherence, the calculated result is decomposed into a one-photon term, a two-photon coherence term contributing to EIT, and a three-photon coherence term contributing to three-photon absorption.

II. EXPERIMENTAL SETUP

The $5S_{1/2}$-$5P_{3/2}$-$5D_{5/2}$ transition of ^{87}Rb has been described under EIT and TPA conditions in a simple three-level ladder-type configuration, as shown in Fig. 1. The EIT and nonresonant TPA due to two-photon coherence are apparently opposite to each other (absorption and transmittance); these phenomena are determined by the branching ratios of three-level ladder-type atomic systems. In Doppler-broadened ladder-type atomic systems, the probe (Ω_p) and coupling (Ω_{C1}) fields overlap and counterpropagate through an Rb atom vapor cell. In this paper, we added a coupling (Ω_{C2}) field, which was counterdirected with respect to Ω_{C1}, to obtain the effect of three-photon coherence. The two counterpropagating coupling fields (Ω_{C1} and Ω_{C2}) are the same as the standing-wave coupling field; however, spatial intensity modulation of the coupling field is not required for the generation of three-photon coherence. Figure 1 shows the three-level atomic system interacting with one probe field (Ω_p) and two counterpropagating coupling fields (Ω_{C1} and Ω_{C2}). However, the energy diagram of a real ladder-type atom is complicated because of the large number of hyperfine states and Zeeman sublevels.

A schematic of the apparatus used in these experiments is shown in Fig. 2. Two external cavity diode lasers (one for the

*Corresponding author: hsmoon@pusan.ac.kr

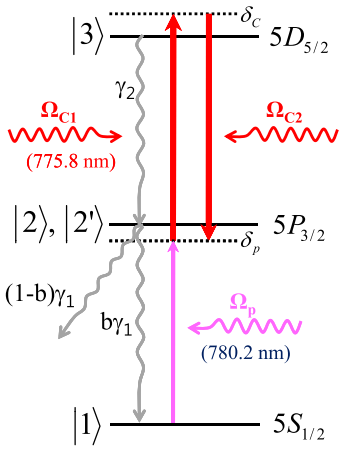

FIG. 1. (Color online) Energy-level diagram for the $5S_{1/2}$-$5P_{3/2}$-$5D_{5/2}$ transitions of ^{87}Rb ($I = 3/2$) showing the probe (Ω_p) and counterpropagating coupling (Ω_{C1} and Ω_{C2}) fields, the decay rates γ_1 ($2\pi \times 6.0$ MHz) and γ_2 ($2\pi \times 0.97$ MHz), the frequency detuning of the probe and coupling laser δ_p and δ_C, and the branching ratios b_1 and b_2.

two coupling fields and the other for the probe field) were independently operated at wavelengths of 776 and 780 nm, respectively. The widths of the two lasers were estimated to be less than 1 MHz. They were linearly polarized in the perpendicular direction, and the intensities of the probe and coupling lasers were 2.7 μW/mm^2 and 3.2 mW/mm^2, respectively. The frequency of the probe laser was scanned over the entire range of excited states in the $5P_{3/2}$ transition, and that of the coupling laser was free running around the $5D_{5/2}$ transition without frequency control. The probe field (Ω_p) was combined with the counterpropagating coupling field (Ω_{C1}) at the polarizing beam splitter (PBS) and the additional coupling field (Ω_{C2}) was aligned with the copropagating probe field using another PBS. We used a Rb vapor cell that was 2.5 cm in diameter and 5 cm in length. To shield the vapor cell from Earth's magnetic field, it was wrapped in three layers of μ-metal sheets. The measured residual magnetic field in the μ-metal chamber was sub-milligauss. The temperature of the vapor cell (room temperature, 23 °C–25 °C) was not controlled. The transmission spectrum of the probe field after it propagated through the vapor cell was measured using a photocurrent detector.

III. EXPERIMENTAL RESULTS

In a real atomic system, there are various transition routes between the hyperfine states. Optical pumping into noninteracting states depends on the spontaneous decay along various paths. The decay rate between the ground and intermediate states significantly affects whether EIT or TPA occurs in a ladder-type atomic system. In this paper, we consider the $5S_{1/2}(F = 2)$-$5P_{3/2}$-$5D_{5/2}$ transition for the EIT condition and the $5S_{1/2}(F = 1)$-$5P_{3/2}$-$5D_{5/2}$ transition for the TPA condition.

Figure 3(a) shows the $5S_{1/2}(F = 2)$-$5P_{3/2}$-$5D_{5/2}$ transitions, in which the $5S_{1/2}(F = 2)$-$5P_{3/2}(F' = 3)$ transition is a cycling transition without population leakage. As is well known, the ladder-type EIT in a Doppler-broadened atomic medium can be achieved only when the probe and coupling fields are counterpropagating, as shown in Fig. 2. When the frequency of the coupling field is free running at the $5P_{3/2}(F' = 3)$-$5D_{5/2}(F'' = 4)$ transition, the hyperfine structures ($F'' = 2, 3, 4$) of the $5D_{5/2}$ state in the ladder-type EIT spectrum due to pure two-photon coherence were easily observed in the presence of the probe (Ω_p) and coupling (Ω_{C1}) fields, as indicated by the blue dashed curve in Fig. 3(b). This is because the hyperfine structures were satisfied under the two-photon resonance conditions, as shown in Fig. 3.

However, when another coupling field (Ω_{C2}) was added under the same conditions as for EIT in Fig. 3(b), strong absorption was observed in the $5D_{5/2}(F'' = 4)$ state instead of the EIT transmittance, as indicated by the red curve in Fig. 3(b). We refer to the enhanced absorption as three-photon electromagnetically induced absorption (TPEIA) because of the three-photon atomic coherence opposing EIT in the hyperfine state of the ladder-type atomic system. If the additional coupling field (Ω_{C2}) is counterpropagated with respect to Ω_{C1}, the three-photon resonance condition for the Doppler-free configuration of the ladder-type TPEIA can be determined to the zero-velocity condition in the configuration shown in Fig. 2. Therefore, the transformation from EIT to TPEIA was observed only in the $5D_{5/2}(F'' = 4)$ state, and the other states $5D_{5/2}(F'' = 2$ and $3)$ remained on the transmittance dips, as

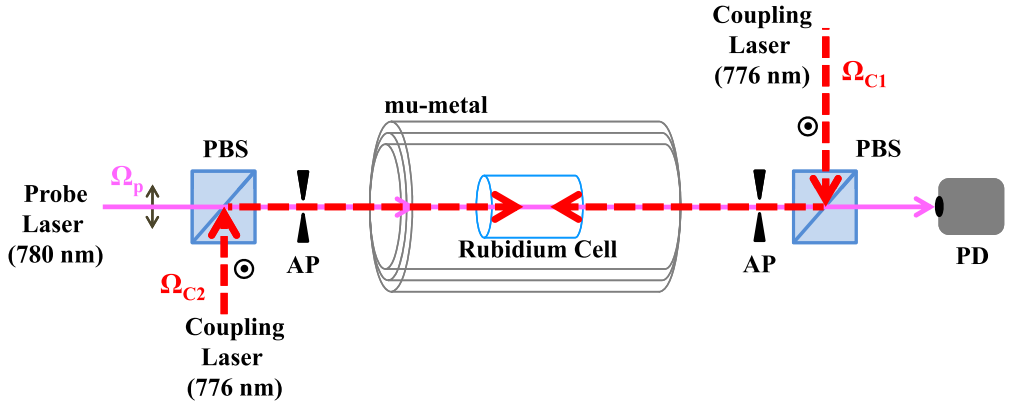

FIG. 2. (Color online) Experimental schematic for the three-photon absorption in the Rb vapor cell (PD: Photo-current detector, PBS: polarization beam splitter, AP: aperture of diameter 1.0 mm).

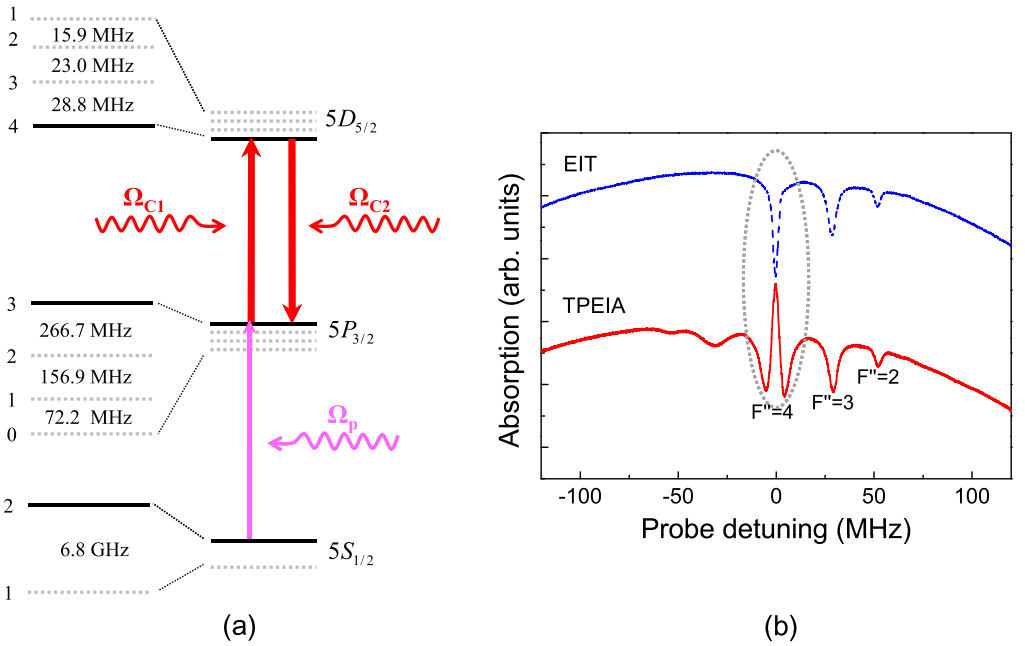

FIG. 3. (Color online) (a) Hyperfine structure of the $5S_{1/2}(F = 2)$-$5P_{3/2}$-$5D_{5/2}$ transition for ladder-type EIT and TPEIA; (b) ladder-type EIT (blue dashed curve) and TPEIA (red curve) spectra for the $5S_{1/2}(F = 2)$-$5P_{3/2}(F' = 3)$-$5D_{5/2}(F'' = 4)$ transition.

indicated by the dashed gray circle in Fig. 3(b). The cause of TPEIA in the ladder-type atomic system will be discussed in detail in the Theoretical Results section.

Interestingly, we observed TPEIA under resonant TPA conditions when the probe laser was resonant with the $5S_{1/2}(F = 1)$-$5P_{3/2}(F' = 2)$ transition, as shown in Fig. 4(a). The atoms in the $5S_{1/2}(F = 1)$ ground state can be optically pumped into the $5S_{1/2}(F = 2)$ ground state and the $5S_{1/2}(F = 1)$-$5P_{3/2}$-$5D_{5/2}$ transition can be described as an open ladder-type atomic system. It is possible to observe the TPA spectrum in the $5S_{1/2}(F = 1)$-$5P_{3/2}$ transition with single resonance optical pumping, as indicated by the blue dashed curve in Fig. 4(b) [25]. When the coupling field (Ω_{C2}) is added under the TPA condition indicated by the blue dashed curve in Fig. 4(b), narrow TPEIA in the $5D_{5/2}(F'' = 3)$ state was observed, as indicated by the red curve in Fig. 4(b). When the frequencies of the two counterpropagating coupling fields are fixed at the $5P_{3/2}(F' = 2)$-$5D_{5/2}(F'' = 3)$ transition,

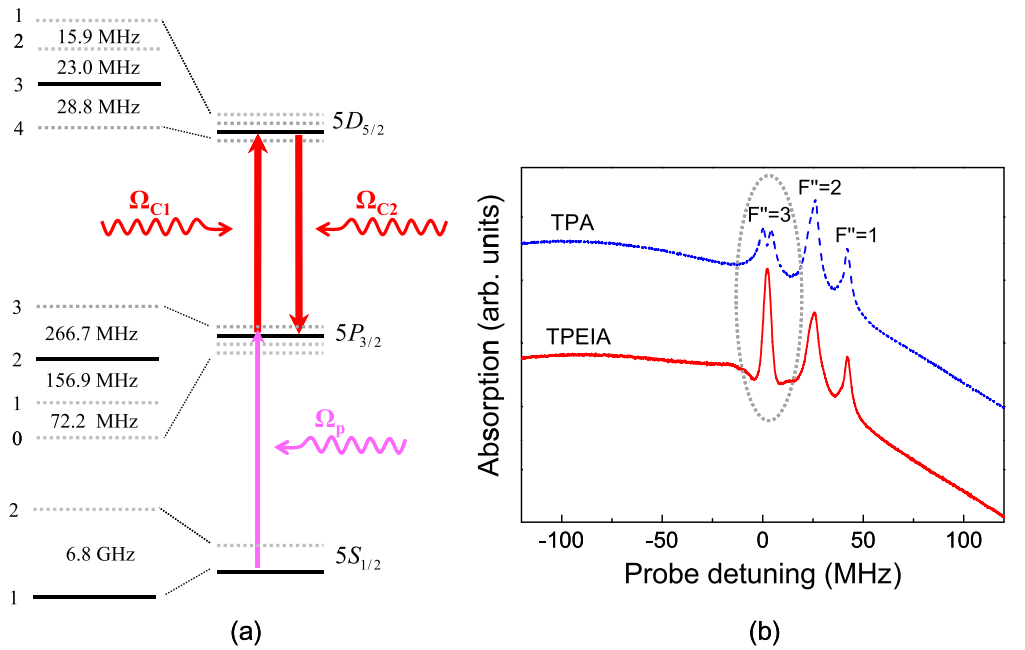

FIG. 4. (Color online) (a) Hyperfine structure of the $5S_{1/2}(F = 1)$-$5P_{3/2}$-$5D_{5/2}$ transition for resonant TPA and TPEIA; (b) the resonant TPA (blue dashed curve) and ladder-type TPEIA (red curve) spectra in the $5S_{1/2}(F = 1)$-$5P_{3/2}(F' = 2)$-$5D_{5/2}(F'' = 3)$ transition.

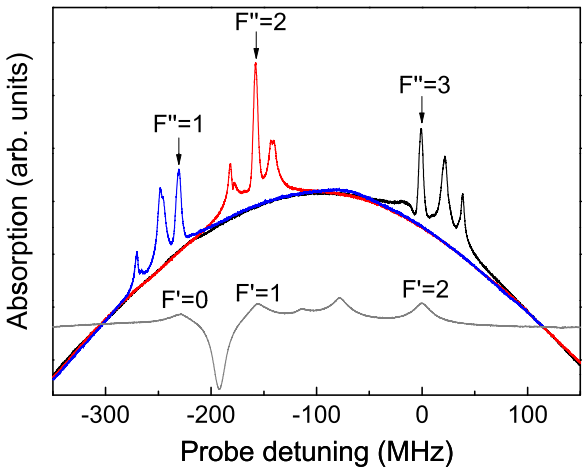

FIG. 5. (Color online) TPEIA spectra based on TPA of the different hyperfine states at the resonances of the $5S_{1/2}(F = 1)$-$5P_{3/2}(F' = 2)$-$5D_{5/2}(F'' = 3)$ (black curve), $5S_{1/2}(F = 1)$-$5P_{3/2}(F' = 1)$-$5D_{5/2}(F'' = 2)$ (red curve), and $5S_{1/2}(F = 1)$-$5P_{3/2}(F' = 0)$-$5D_{5/2}(F'' = 1)$ (blue curve) transitions.

the Doppler-free configuration of the ladder-type TPEIA was observed only in the $5D_{5/2}(F'' = 3)$ state, and the absorption of the other states $5D_{5/2}(F'' = 1$ and $2)$ was not changed.

We investigated TPEIA in the different hyperfine states, as shown in Fig. 5. The black, red, and blue curves show the absorption spectra as a function of the coupling field frequency when the coupling field frequencies are tuned to the resonant frequencies of the $5P_{3/2}(F' = 2)$-$5D_{5/2}(F'' = 3)$, $5P_{3/2}(F' = 1)$-$5D_{5/2}(F'' = 2)$, and $5P_{3/2}(F' = 0)$-$5D_{5/2}(F'' = 1)$ transitions, respectively. Here, the gray curve represents the saturated absorption spectrum obtained using the probe laser. When the frequency of the probe field satisfied the three-photon resonance condition in the Doppler-broadened ladder-type atomic system, the TPEIA peaks of the absorption spectra were clearly observed. This means that the three-photon resonance condition is not satisfied for moving atoms. As a result of the velocity selective effect, the TPEIA spectra are due only to atoms in the region of zero velocity with respect to the direction of laser propagation. The laser frequencies of the two counterpropagating coupling fields in the moving atoms differed because of the Doppler effect. Therefore, we assert that the TPEIA spectrum under TPA conditions was caused primarily by three-photon coherence in the ladder-type atomic system with the additional coupling field.

IV. THEORETICAL RESULTS

To interpret ladder-type TPEIA under both EIT and resonant TPA conditions, we assumed a modified three-level atomic system considering three-photon coherence, as shown in Fig. 1. This system, which is effective for analyzing three-photon coherence in ladder-type atomic systems, consists of a ground state ($|1\rangle$), intermediate states ($|2\rangle$ and $|2'\rangle$), and an excited state ($|3\rangle$). The probe field is tuned to the $|1\rangle \leftrightarrow |2\rangle$ transition and the two coupling fields are tuned to the $|2\rangle \leftrightarrow |3\rangle$ and $|2'\rangle \leftrightarrow |3\rangle$ transitions, respectively.

We solved the density-matrix equations for the modified three-level atomic system, which was derived from the time-dependent Schrödinger equation. The time evolution of the density matrix is given by the optical Bloch equation as follows:

$$\frac{\partial\hat{\rho}}{\partial t} = \frac{1}{i\hbar}[H_0 + H_{\rm int}, \hat{\rho}] + \frac{\partial\hat{\rho}_{\rm sp}}{\partial t}, \tag{1}$$

where $\hat{\rho}$ is a density-matrix element, and H_0 and $H_{\rm int}$ are the atomic and interaction Hamiltonians, respectively. $\frac{\partial\hat{\rho}_{\rm sp}}{\partial t}$ is the relaxation term describing all the relaxation processes. In Fig. 1, the decay rate γ_1 from the intermediate state to the ground state is $2\pi \times 6.0$ MHz and the decay rate γ_2 from the excited state to the intermediate state is $2\pi \times 0.97$ MHz. The density-matrix equations for the three-level system considering three-photon coherence are given by

$$\dot{\rho}_{11} = \frac{1}{2}b_1\gamma_1(\rho_{22} + \rho_{2'2'}) - \Omega_p {\rm Im}\rho_{12}, \tag{2a}$$

$$\dot{\rho}_{22} = \frac{1}{2}b_2\gamma_2\rho_{33} - \frac{1}{2}\gamma_1\rho_{22} + \Omega_p {\rm Im}\rho_{12} - \Omega_{C1}{\rm Im}\rho_{23}, \tag{2b}$$

$$\dot{\rho}_{2'2'} = \frac{1}{2}b_2\gamma_2\rho_{33} - \frac{1}{2}\gamma_1\rho_{22} + \Omega_{C2}{\rm Im}\rho_{32'}, \tag{2c}$$

$$\dot{\rho}_{33} = -\gamma_2\rho_{33} + \Omega_{C1}{\rm Im}\rho_{23} - \Omega_{C2}{\rm Im}\rho_{32'}, \tag{2d}$$

$$\dot{\rho}_{12} = \frac{i}{2}\left[-2\delta_1\rho_{12} + \frac{i}{2}\gamma_1\rho_{12} + \Omega_{C1}\rho_{13} - \Omega_p(\rho_{22} - \rho_{11})\right], \tag{2e}$$

$$\dot{\rho}_{13} = \frac{i}{2}\Big[-2(\delta_1 + \delta_2)\rho_{13} + i\gamma_2\rho_{13} - \Omega_p\rho_{23} + \Omega_{C1}\rho_{12} + \Omega_{C2}\rho_{12'}\Big], \tag{2f}$$

$$\dot{\rho}_{12'} = \frac{i}{2}\Big[2(-\delta_1 - \delta_2 + \delta_3)\rho_{12'} + \frac{i}{2}\gamma_1\rho_{12'} - \Omega_p\rho_{22'} + \Omega_{C2}\rho_{13}\Big], \tag{2g}$$

$$\dot{\rho}_{23} = \frac{i}{2}\Big[-2\delta_2\rho_{23} + \frac{i}{2}(\gamma_1 + 2\gamma_2)\rho_{23} - \Omega_p\rho_{13} + \Omega_{C1}(\rho_{22} - \rho_{33}) + \Omega_{C2}\rho_{22'}\Big], \tag{2h}$$

$$\dot{\rho}_{22'} = \frac{i}{2}\Big[2(\delta_3 - \delta_2)\rho_{22'} + \frac{i}{2}(\gamma_1 + \gamma_2)\rho_{22'} - \Omega_p\rho_{12'} - \Omega_{C1}\rho_{32'} + \Omega_{C2}\rho_{23}\Big], \tag{2i}$$

$$\dot{\rho}_{32'} = \frac{i}{2}\Big[2\delta_3\rho_{32'} + \frac{i}{2}(\gamma_1 + 2\gamma_2)\rho_{22'} - \Omega_{C1}\rho_{22'} + \Omega_{C2}(\rho_{22} - \rho_{2'2'})\Big], \tag{2j}$$

where $\delta_1 = \delta_{\rm p} - (2\pi/\lambda_1)v$ and $\delta_{2(3)} = \delta_{\rm C} \pm (2\pi/\lambda_2)v$. Here, $\delta_{\rm p}$ and $\delta_{\rm C}$ arethe frequency detuning of the probe and coupling laser, respectively. We assumed the branching ratios b_1 and b_2 to consider the conditions of EIT and resonant TPA [28].

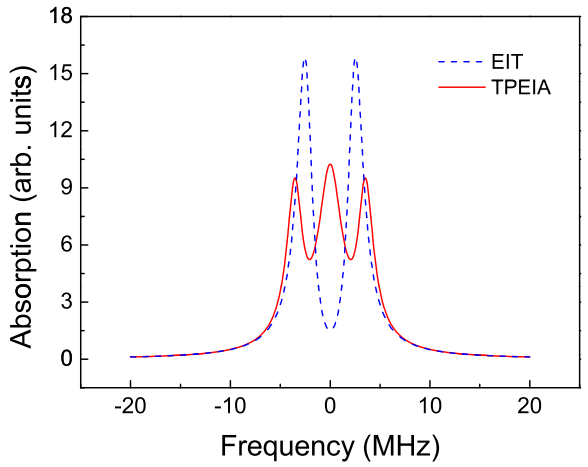

FIG. 6. (Color online) Numerically calculated EIT (blue dashed curve) and TPEIA (red curve) spectra in the case of motionless ladder-type three-level atomic system.

Using the modified three-level atomic system considering three-photon coherence, we calculated the EIT and TPEIA spectra in the case of a motionless atomic system without Doppler broadening, as shown in Fig. 6, where the branching ratios are set to $b_1 = 1$ and $b_2 = 0.75$. The blue dashed curve of Fig. 6 shows the typical EIT spectrum of stopped atoms when the Rabi frequencies of the probe field (Ω_p) and the coupling field (Ω_{C1}) are 0.3 and 5.0 MHz, respectively. When another coupling field (Ω_{C2}) of 4.0 MHz is added in the modified three-level atomic system considering three-photon coherence, we can obtain the TPEIA signal at resonance, as shown in the red curve of Fig. 6. In this case, the directions of the two coupling and probe fields were not considered. Therefore, the modified three-level atomic system considering three-photon coherence is the appropriate model for understanding a transformation between EIT and TPEIA in the case of motionless ladder-type atomic system.

Depending upon the branching ratios, Figs. 7(a) and 7(b) show the calculated spectra of EIT and TPEIA with $b_1 = 1$ and $b_2 = 0.75$, and of TPA and TPEIA with $b_1 = 0.5$ and $b_2 = 0.5$, respectively [29]. To consider the Doppler-broadened ladder-type atomic system, the numerical results of the density matrix were averaged over the Maxwell-Boltzmann velocity distribution. The parameters for the numerical calculations are as follows: Ω_p, Ω_{C1}, and Ω_{C2} are 0.3, 5.0, and 4.0 MHz, respectively. The blue dashed curve in Fig. 7(a) shows the calculated EIT spectrum under the condition of ladder-type EIT of the $5S_{1/2}(F = 2)$-$5P_{3/2}(F' = 3)$-$5D_{5/2}(F'' = 4)$ transition, which is similar to the experimental results shown in Fig. 3(b). When three-photon coherence was considered with respect to another coupling field (Ω_{C2}) under EIT conditions, the TPEIA spectrum [the red curve in Fig. 7(a)] was calculated. In the Doppler-broadened ladder-type atomic system, Ω_{C2}, which copropagates with Ω_p, is not Doppler free for the two-photon resonance condition; it is, however, Doppler free for the three-photon resonance condition.

The blue dashed curve in Fig. 7(b) represents the calculated resonant TPA spectrum without Ω_{C2}. When the three-photon coherence was generated using another coupling field (Ω_{C2}), the TPEIA was calculated under TPA conditions, as shown by the red curve in Fig. 6(b). Although the magnitudes of EIT and TPA are smaller than that of TPEIA, the calculated TPEIA spectra (red curves) in Figs. 7(a) and 7(b) are in good agreement with the experimental results given in Figs. 3 and 4.

For a detailed understanding of the origin of ladder-type TPEIA under both EIT and TPA conditions, the calculated TPEIA spectra were decomposed into one-photon, two-photon, and three-photon resonance components, as shown in Fig. 8. The one-photon resonance effect was calculated using the density-matrix equation when the two-photon and three-photon coherence components were set to zero. To obtain the three-photon resonance effect, the one-photon and two-photon signals were first calculated by setting the three-photon coherence term to zero. The three-photon coherence effect was then obtained by subtracting the one-photon and two-photon signals from the total TPEIA spectrum.

As shown in Figs. 8(a) and 8(b), the calculated one-photon resonance component (blue dashed curves) is broad and weak compared to the components related to the one-photon absorption and Doppler-broadening effects. For the

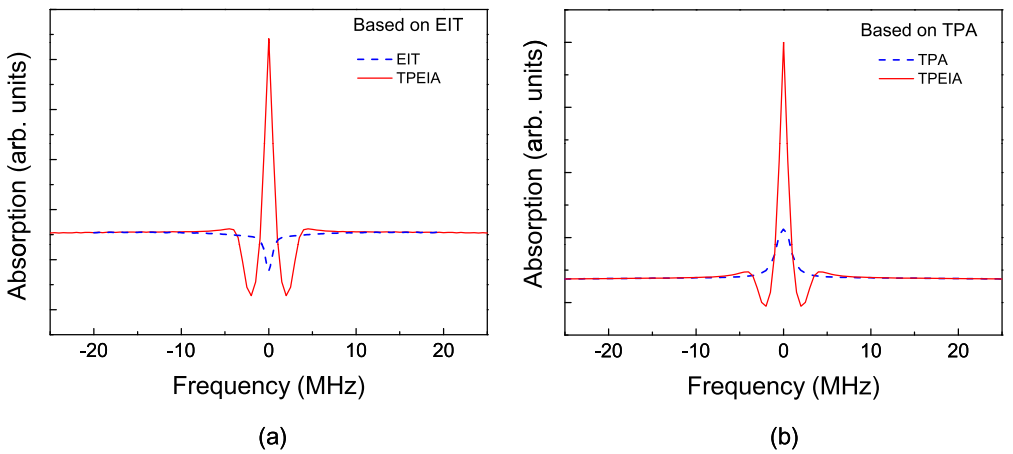

FIG. 7. (Color online) Numerically calculated spectra in the ladder-type three-level atomic system for the three-photon coherence; (a) the EIT (blue dashed curve) and TPEIA (red curve) with $b_1 = 1$ and $b_2 = 0.75$, and (b) the TPA (blue dashed curve) and TPEIA (red curve) with $b_1 = 0.5$ and $b_2 = 0.5$.

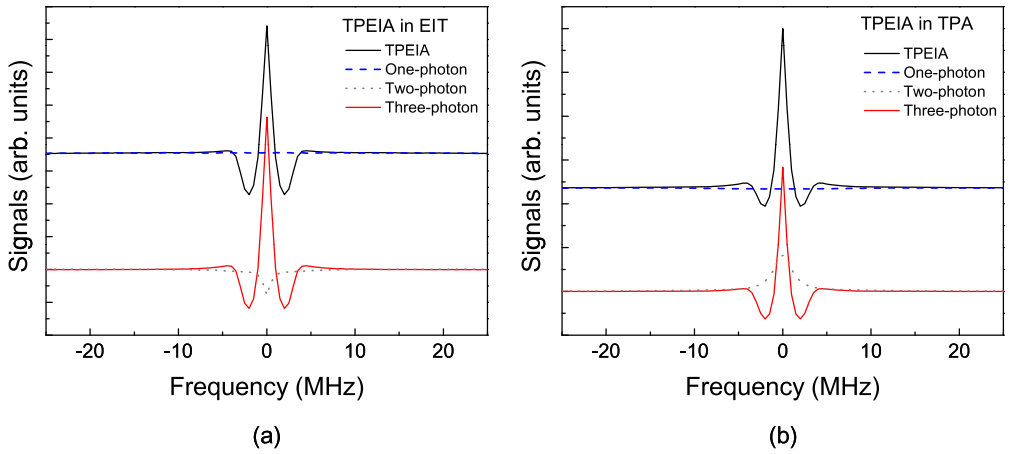

FIG. 8. (Color online) Decomposition of the ladder-type TPEIA spectra into the one-photon (blue dashed curve), two-photon (gray dotted curve), and three-photon (red curve) resonance terms: (a) EIT and (b) resonant TPA conditions.

two-photon resonance component, the gray dotted curves in Figs. 8(a) and 8(b) show the EIT and TPA spectra, respectively. The EIT and TPA components change significantly depending on the branching ratio [25]. When the branching ratios are set to $b_1 = 1$ and $b_2 = 0.75$, the two-photon resonance effect is more dominant in the TPA component than in the EIT component, as shown in Fig. 8(a). However, when the branching ratios are set to $b_1 = 0.5$ and $b_2 = 0.5$, the TPA component dominates in the two-photon resonance effect of Fig. 8(b). In contrast, the narrow absorption signals (red curves), which are due to three-photon coherence, contributed significantly to TPEIA at resonance for both EIT and TPA, as shown in Figs. 8(a) and 8(b). It can be observed that the main cause of the induced absorption in the three-photon resonance is three-photon coherence. The three-photon resonance condition in the homogeneously broadened ladder-type atomic system is satisfied using the configuration of the probe and two counterpropagating coupling fields, as shown in Fig. 2. In particular, in comparison with the typical EIA due to spontaneous coherence transfer, the absorption in TPEIA based on TPA in the ladder-type atomic system significantly exceeds linear absorption. Therefore, ladder-type TPEIA is an interesting phenomenon due to quantum coherence effects resulting from three-photon coherence.

V. CONCLUSION

We studied ladder-type TPEIA based on EIT and resonant TPA for the $5S_{1/2}$-$5P_{3/2}$-$5D_{5/2}$ transition of ^{87}Rb atoms. When the probe and two counterpropagating coupling fields interacted with Rb atoms, the transformation of EIT and TPA to TPEIA was observed in Doppler-broadened ladder-type atomic systems. Because only atoms in the region of zero velocity satisfy the three-photon resonance condition, only one of the hyperfine structures was observed in the TPEIA, and the other states remained under EIT and TPA. By changing the frequencies of the coupling fields, we observed TPEIA of the different hyperfine states for three-photon resonance. Using the modified three-level atomic system considering three-photon coherence, we numerically calculated the TPEIA spectra under the TPA and EIT conditions, which were then decomposed into one-photon, two-photon, and three-photon terms. From the calculated results, we could see that the main cause of the ladder-type TPEIA was three-photon coherence under both TPA and EIT conditions. The observed spectra were shown to be in good agreement with the numerical calculations. Our experimental and calculated results are expected to provide a better understanding of multiphoton coherence effects in three-level ladder-type atomic systems.

ACKNOWLEDGMENTS

This research was supported by Basic Science Research Program through the National Research Foundation of Korea (NRF) funded by the Ministry of Education, Science and Technology (Grant No. 2012R1A2A1A01006579). Also, this work was supported by the Measurement Research Center (MRC) Program for Korea Research Institute of Standards and Science.

[1] K. J. Boller, A. Imamoglu, and S. E. Harris, Phys. Rev. Lett. **66**, 2593 (1991).
[2] S. E. Harris, Phys. Today **50**, 36 (1997).
[3] M. Xiao, Y. Q. Li, S. Z. Jin, and J. Gea-Banacloche, Phys. Rev. Lett. **74**, 666 (1995).
[4] A. M. Akulshin, S. Barreiro, and A. Lezama, Phys. Rev. A **57**, 2996 (1998).
[5] J. Gea-Banacloche, Y. Q. Li, S. Z. Jin, and M. Xiao, Phys. Rev. A **51**, 576 (1995).
[6] A. V. Taichenachev, A. M. Tumaikin, and V. I. Yudin, Phys. Rev. A **61**, 011802 (1999).
[7] C. Liu, Z. Dutton, C. H. Behroozi, and L. V. Hau, Nature **409**, 490 (2001).
[8] J. Vanier, Appl. Phys. B **81**, 421 (2005).

[9] D. Budker and M. V. Romalis, Nat. Phys. **3**, 227 (2007).
[10] H. S. Moon, L. Lee, K. Kim, and J. B. Kim, Appl. Phys. Lett. **84**, 3001 (2004).
[11] I.-H. Bae and H. S. Moon, Phys. Rev. A **83**, 053806 (2011).
[12] S. Wielandy and A. L. Gaeta, Phys. Rev. A **58**, 2500 (1998).
[13] S. D. Badger, I. G. Hughes, and C. S. Adams, J. Phys. B **34**, L749 (2001).
[14] A. K. Mohapatra, T. R. Jackson, and C. S. Adams, Phys. Rev. Lett. **98**, 113003 (2007).
[15] H. S. Moon, L. Lee, and J. B. Kim, Opt. Express **16**, 12163 (2008).
[16] M. A. Kumar and S. Singh, Phys. Rev. A **79**, 063821 (2009).
[17] C. Liu, J. F. Chen, S. Zhang, S. Zhou, Y.-H. Kim, M. M. T. Loy, G. K. L. Wong, and S. Du, Phys. Rev. A **85**, 021803 (2012).
[18] H. S. Moon and H.-R. Noh, Opt. Express **21**, 7447 (2013).
[19] K. Pandey, Phys. Rev. A **87**, 043838 (2013).
[20] C. Affolderbach, S. Knappe, R. Wynands, A. V. Tavĭchenachev, and V. I. Yudin, Phys. Rev. A **65**, 043810 (2002).
[21] I.-H. Bae, H. S. Moon, M.-K. Kim, L. Lee, and J. B. Kim, Opt. Express **18**, 1389 (2010).
[22] H. Y. Ling, Y. Q. Li, and M. Xiao, Phys. Rev. A **57**, 1338 (1998).
[23] A. André and M. D. Lukin, Phys. Rev. Lett. **89**, 143602 (2002).
[24] D. V. Strekalov, A. B. Matsko, and N. Yu, Phys. Rev. A **76**, 053828 (2007).
[25] S. A. Babin, D. V. Churkin, E. V. Podivilov, V. V. Potapov, and D. A. Shapiro, Phys. Rev. A **67**, 043808 (2003).
[26] A. M. Akulshin, R. J. McLean, A. I. Sidorov, and P. Hannaford, J. Phys. B **44**, 175502 (2011).
[27] A. M. Akulshin, A. Cimmino, A. I. Sidorov, R. J. McLean, and P. Hannaford, J. Opt. B: Quantum Semiclassical Opt. **5**, S479 (2003).
[28] H.-R. Noh and H. S. Moon, Opt. Express **19**, 11128 (2011).
[29] H.-R. Noh and H. S. Moon, Phys. Rev. A **85**, 033817 (2012).